computation

MDPI

Article

Theoretical Prediction of Electronic Structures and Phonon Dispersion of Ce_2XN_2 (X = S, Se, and Te) Ternary

Mohammed Benali Kanoun * and Souraya Goumri-Said *

College of Science, Department of Physics, Alfaisal University, P.O. Box 50927 Riyadh, Saudi Arabia
* Correspondence: mkanoun@alfaisal.edu (M.B.K.) and sosaid@alfaisal.edul (S.G.-S.); Tel.: +966112157802

Academic Editor: Jianmin Tao
Received: 24 March 2017; Accepted: 30 May 2017; Published: 13 June 2017

Abstract: A systematic study of structural, electronic, vibrational properties of new ternary dicerium selenide dinitride, Ce_2SeN_2 and predicted compounds—Ce_2SN_2 and Ce_2TeN_2—is performed using first-principles calculations within Perdew–Burke–Ernzerhof functional with Hubbard correction. Our calculated results for structural parameters nicely agree to the experimental measurements. We predict that all ternary dicerium chalcogenide nitrides are thermodynamically stable. The predicted elastic constants and related mechanical properties demonstrate its profound mechanical stability as well. Moreover, our results show that Ce_2XN_2 are insulator materials. Trends of the structural parameters, electronic structures, and phonon dispersion are discussed in terms of the characteristics of the Ce (4f) states.

Keywords: dicerium chalcogenide nitrides; DFT+U calculations; electronic structures; phonon dispersion

1. Introduction

In recent years, remarkable progress has been made in the field of synthesis of novel multinary nitrides. They are known to exhibit a wide variety of physical properties as well as magnetic, electronic, optical, and catalytic properties [1–4]. Exploring their structure–bonding properties relationships remains the priority of many scientists in the field of solid-state chemistry [5]. Important works toward understanding structural diversity and complexity of lanthanide compounds have been made by Schleid and co-workers [6,7]. It was suggested that this heteroanionic system possesses a structural versatility comparable to that of oxynitrides and nitride halides. This area has been also extended to Li containing chalcogenide nitrides [8] to find new fast ion conductors with trivalent cations. Moreover, ternary compounds based on lanthanoid chalcogenide nitrides exhibit surprising crystal structures [7], whereas the binary rocksalt-type mononitrides LnN [7] display octahedrally surrounded cations and anions.

Recently, DiSalvo and co-workers introduced a new phase containing a tetravalent cation [9,10]. Subsequently, Dong and DiSalvo [11] synthesized a new ternary dicerium selenide dinitride using single crystal X-ray structure determination. Thus, to support the experimental findings reported by Dong and DiSalvo [11], we investigated using first-principles based methods to study the structural and electronic properties of the new ternary Ce_2SeN_2. We have also extended our theoretical works on the Ce_2SN_2 and Ce_2TeN_2 ternary phases in order to predict their crystal parameters, electronic structures, bonding characterization, and phonon dispersion. The role of changing X (= S, Se, or Te) on the structural properties and electronic structures as well as the bonding properties within the series of 2:1:2 compounds can be addressed from comparative analyses of the charges and formation

energies. The purpose of this work is to present such a detail study for the Ce_2XN_2 ternaries with *X* = S, Se, or Te.

2. Computational Details

The total energy and electronic structure have been calculated within the density functional formalism using the projector augmented wave (PAW) approach [12] as implemented in the Vienna ab initio Simulation Package (VASP) [13]. The interaction between the core electrons and the valence electrons is described with the projector augmented wave potentials. The Perdew–Burke–Ernzerhof (PBE) [14] version of the generalized gradient approximation (GGA) is used for the exchange-correlation potential. On-site Hubbard interaction between the highly localized 5f electrons was treated within the rotationally invariant form [15] of GGA + *U*, a combination of the standard GGA and a Hubbard parameter *U*. The effective on-site Coulomb interaction energy *U* (*U* − J), is applied to the Ce 5f electrons (6 eV and 1 eV, respectively), as suggested in [16]. A plane waves energy cutoff of 500 eV was used. Structure relaxations were performed with 8 × 8 × 4 k-point grids, while the electronic properties were calculated by 16 × 16 × 8 k-point grids in the Monkhorst–Pack scheme [17]. During the geometry optimizations, all atoms were allowed to relax until the Hellmann–Feynman forces were smaller than 0.01 eV/Å. Both lattice vectors and atomic positions were fully relaxed. From the calculation, we determined the trends of electronic charge transfers by means of the analysis of the charge density obtained from the self-consistent calculations using the (AIM) theory approach [18] developed by Bader who devised an intuitive way of separating molecules into element atoms as based purely on the electronic charge density.

3. Results and Discussion

The new ternary dicerium selenide dinitride, Ce_2SeN_2, crystallizes in the trigonal space group *P-31m* (No. 157). The unit cell parameters were found to be *a* = 4.0772(3) Å, *c* = 7.0477(7) Å, with $\alpha = \beta = 90$ and $\gamma = 120$ [11] with Z = 1. Projections of the Ce_2SeN_2 structure are presented in Figure 1. The crystal structure is built up of Ce atoms forming a hexagonal closed packing along the c-axis. The Se atoms occupy all the octahedral voids between every other pair of Ce layers, while the N atoms fill all the tetrahedral voids between the remaining pairs of Ce layers. In addition, each Ce atom is surrounded by three Se atoms and four N atoms [11] (see Figure 1). However, in this work, we also extended our calculation to study the hypothetical compounds like Ce_2SN_2 and Ce_2TeN_2.

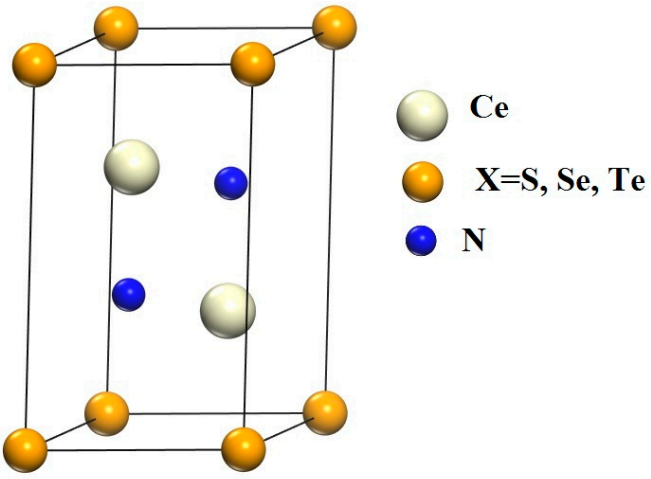

Figure 1. The unit cell structure of trigonal of Ce_2XN_2.

The crystal structure contains variable internal coordinates characterizing the 2:1:2 trigonal structure, namely z_{Ce} and z_N whereby Ce is found at (2d) 1/3, 2/3, z_{Ce} with z_{Ce} = 0.7153 and N at (1a) 1/3, 2/3, z_N with 1/3, 2/3, z_N = 0.3744 while X = S, Se, and Te is at (2a) 0, 0, 0 (the experimental lattice

and positional parameters can be found in the original literature [11]). Full geometry optimization of all three ternaries showed a preserved crystal symmetry and space group positions and calculated z_{Ce} and z_N changed by less than 2%. The relaxed structural parameters are reported in Table 1 along with the experimental results and displayed in Figure 2. In Table 1, it was found that our calculated bond lengths agree well with the experimental data [9]. Our results show that the *a* is very close, the difference is better observed for *c*. The trends can be seen more easily: on going from Ce_2SN_2 to Ce_2SeN_2 to Ce_2TeN_2, it is seen that the lattice constants increase (see Figure 2); the increase of electrons number of the chalcogen elements when moving down along the columns of periodic table results in an increase of the lattice parameters. The lattice constant shows an increase in accordance with the large size of the chalcogen atom.

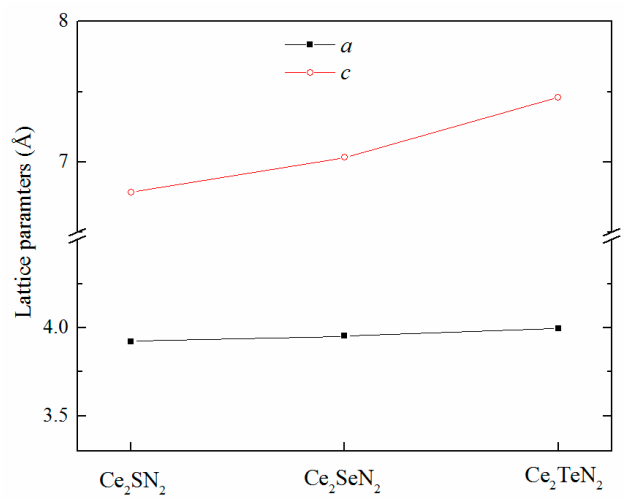

Figure 2. Lattice parameters for ternary dicerium dinitrides.

Table 1. Calculated structural parameters, *a*, *c*, relaxed atomic parameters, *z*, formation energy, ΔE_f, and charges, *Q of* Ce_2SN_2, Ce_2SeN_2, and Ce_2TeN_2 compounds. The elastic constants C_{ij}, bulk modulus B_H, shear modulus, G_H, and Young's modulus, *E*, are also shown.

	Ce_2SeN_2		**Ce_2SN_2**	**Ce_2TeN_2**
	This work	Exp. [11]	This work	
a (Å)	3.953	4.077	3.923	3.996
c (Å)	7.032	7.047	6.785	7.461
$z_{Ce,N}$	z_{Ce} = 0.7026 z_N = 0.3716	z_{Ce} = 0.7153 z_N = 0.3744	z_{Ce} = 0.7115 z_N = 0.3681	z_{Ce} = 0.7115 z_N = 0.3681
ΔE_f (eV)	−2.56		−3.65	−2.58
Q (e)	Q_{Ce} = +1.96 Q_{Se} = −0.99 Q_N = −1.46		Q_{Ce} = +1.99 Q_S = −1.07 Q_N = −1.45	Q_{Ce} = +1.84 Q_{Te} = −0.56 Q_N = −1.56
C_{11} (GPa)	202.9		220.8	183.6
C_{12} (GPa)	94.3		93.7	86.3
C_{13} (GPa)	75.1		72.4	83.9
C_{14} (GPa)	2.9		1.0	6.3
C_{33} (GPa)	185.7		184.5	207.0
C_{44} (GPa)	80.6		84.8	76.1
B_H (GPa)	119.7		121.6	120.1
G_H (GPa)	65.1		71.7	60.0
E (GPa)	165.3		179.7	154.3

We then extracted the formation energies and the charge transfers of the different compounds from our theoretical calculations. The latter are computed from the charge density analysis with the AIM theory presented above, as reported in Table 1. The charge analysis shows that Ce is the most electropositive elements whereas S, Se, Te, and N elements are more electronegative. The formation energy, ΔE_f, was calculated using the following formulation [19]:

$$\Delta E_f = E_{tot}(Ce_2XN_2) - \frac{1}{2}\left[E_{tot}(Ce) + E_{tot}(X) + \frac{1}{2}E_{tot}(N_2)\right] \quad (1)$$

Here $E_{tot}(Ce_2XN_2)$ is the total energy of the Ce_2XN_2 and, $E_{tot}(Ce)$, $E_{tot}(X)$ and $E_{tot}(N_2)$ represent the isolated atomic energies of the individual metal species in crystalline form and molecular nitrogen N_2, respectively. Our calculated formation energy values are also reported in Table 1. The formation energy values are negative, indicating their intrinsic stability.

To investigate the strength and mechanical stability of Ce_2XN_2, we calculated the stiffness elastic constants C_{ij}, as shown in Table 1. The elastic stability is checked by the whole set of elastic stiffness constants that satisfies the Born–Huang criterion [20] defined for trigonal structure, i.e., $C_{11} > |C_{12}|$, $(C_{11} + C_{12})C_{33} > 2C_{13}^2$, $(C_{11} - C_{12})C_{44} > 2C_{14}^2$. After obtaining elastic constants, the polycrystalline bulk modulus (B_H), shear modulus (G_H), Young's modulus (E), and Poisson's ratio (ν) are calculated from the Voigt–Reuss–Hill (VRH) approximations [21,22]. The calculated polycrystalline elastic constants of ternary nitrides are summarized in Table 1. We notice that Ce_2XN_2 ternaries exhibit a large value of C_{11} and a small value of C_{44}, implying a low G_H and E despite diving a relatively large B_H.

In order to explain the electronic structure of new ternaries Ce_2XN_2 with X = S, Se, and Te, we calculated the total and projected densities of state curves at the predicted equilibrium lattice constants within the frame work of GGA + U, as shown in Figure 3. The vertical line is the Fermi level (E_F). It can be seen from total DOS graphs that the effect of U on the electronic properties is essentially limited to the unoccupied f band and this does not change the electronic structures especially occupied states [16]. The overall DOS profiles are almost similar for all compounds. Our predicted results indicate that Ce_2XN_2 are an insulator. The PDOS shows several interesting features. At the bottom of the valence band—i.e., between −20 and −15 eV—the first valence band is involved essentially from the N s states. The next bands occur between −13 and −10 eV is mostly due to N s and S/Se/Te s states. The region at the bottom of the valence-band, i.e., between −13 and −8 eV, is originated from S/Se/Te p states and Ce 5d states. The upper region of the valence-band is mostly dominated by N 2p states with contributions of S/Se/Te p states and Ce f states, whereas the narrow empty band situated above the Fermi level is dominated by unoccupied Ce 4f. It can be observed that the N 2p states hybridize strongly with the S/Se/Te p states. The respective energy gaps between the valance-band top and the unoccupied Ce 4f (Ce 5d) band bottom show that the three ternaries are insulating with gap magnitudes of 1.16 eV (2.60 eV), 1.08 (2.43 eV), and 0.35 eV (2.08 eV) for Ce_2SN_2, Ce_2SeN_2, and Ce_2TeN_2 respectively. The calculated electronic structures show that bandgap decreases as atomic number increases from S to Se to Te elements.

The bonding characteristics with Ce_2XN_2 ternary are discussed based on the charge density difference map, as shown in Figure 4. This is calculated by subtracting the electron density of Ce, (S, Se, and Te) and N atoms rigidly separated in the geometry they have in total ternary system [23–25]. At self-consistent energy calculations, the charge transfer is from Ce towards N and X in Ce_2XN_2 in agreement with the above computed quantities using the charge density analysis. Similar behavior is observed in the case of CeO_2 [16]. We also show for all compounds that the Ce–N bonds have a strong ionic character as well as a covalent nature due to the interaction between Ce f/X p and N p orbitals. We conclude that ionic bonding is the main determinant of the chemical bonding in Ce_2XN_2, although the covalency is stronger in the sense of orbital participation in forming the valence state.

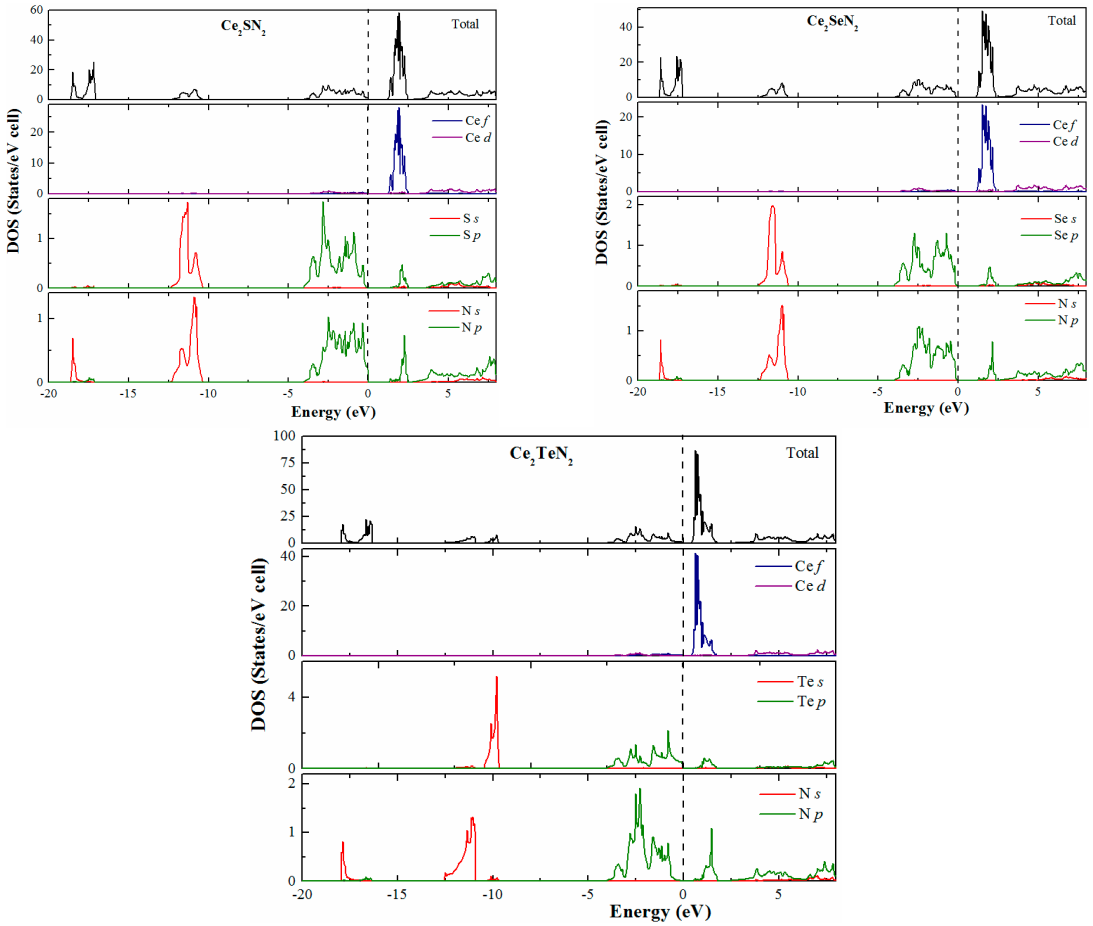

Figure 3. Calculated total and partial densities of states (DOS) for Ce_2SN_2, Ce_2SeN_2, and Ce_2TeN_2. The line at zero is the Fermi level.

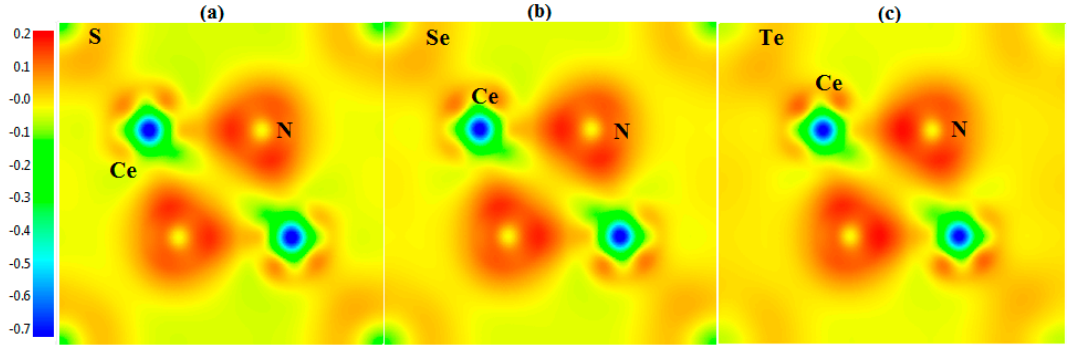

Figure 4. Charge density difference map in the (110) plane shown for (**a**) Ce_2SN_2, (**b**) Ce_2SeN_2, and (**c**) Ce_2TeN_2, (color scale units are electrons/Å^3).

Ce_2XN_2 has symmetry group of *P*-3*m*1 (No. 164), its point group is D_{3d} (−3m). In the standard notation, the mechanical representation can lead to distinguish of acoustic and optic active modes as: $M = 2A_{1g} + 3A_{2u} + 3E_u + 2E_g$, where two acoustic modes are centered in Γ as $\Gamma_{acoustic} = A_{2u} + E_u$ and eight optic mode as: $\Gamma_{optic} = 2A_{1g} + 2A_{2u} + 2E_u + 2E_g$. From these modes, three infrared are active modes: $2A_{2u} + 2E_u$ (Acoustic modes not included) and three Raman modes are active as: $2A_{1g} + 2E_g$. When, we employ the polarization selection rules for Raman and Hyper-Raman processes, we found the following Hyper-Raman active modes: $2A_{2u} + 2E_u$ (Acoustic modes not included). Calculations of the lattice dynamics of the present nitrides within the first-principles calculations give rich information about the phonon eigenmodes and might be used to support the assignment of the experimentally observed features in the Raman and infrared spectra, when available in the future. In the present work, the calculations of the total energy and Hellmann–Feynman forces were carried out using the

CASTEP [26,27]. Vanderbilt ultrasoft pseudopotentials were used to describe the ionic cores. The GGA with PBE [14] functional is adopted. The plane-wave cutoff energy was set at 400 eV. The Brillouin zone integration was sampled using 8 × 8 × 4 k-point grid. We calculated the phonon dispersion relations for Ce_2XN_2 by using the Hellmann–Feynman forces in the small displacement along the optimized structures with the ground-state energy, as shown in Figure 5. In the present calculation, the maximal magnitude of the Hellmann–Feynman forces is less than 0.0004 eV/Å. At Γ point, we observe LO–TO splitting induced by the coupling of phonon modes and the electric field. Furthermore, from all the dispersion curves, no imaginary phonon frequency was observed in the considered BZ which confirms the dynamic stability of the considered nitrides. A large phonon band gap with 175 cm^{-1}, centered on 350 cm^{-1}, is evident for all three nitrides.

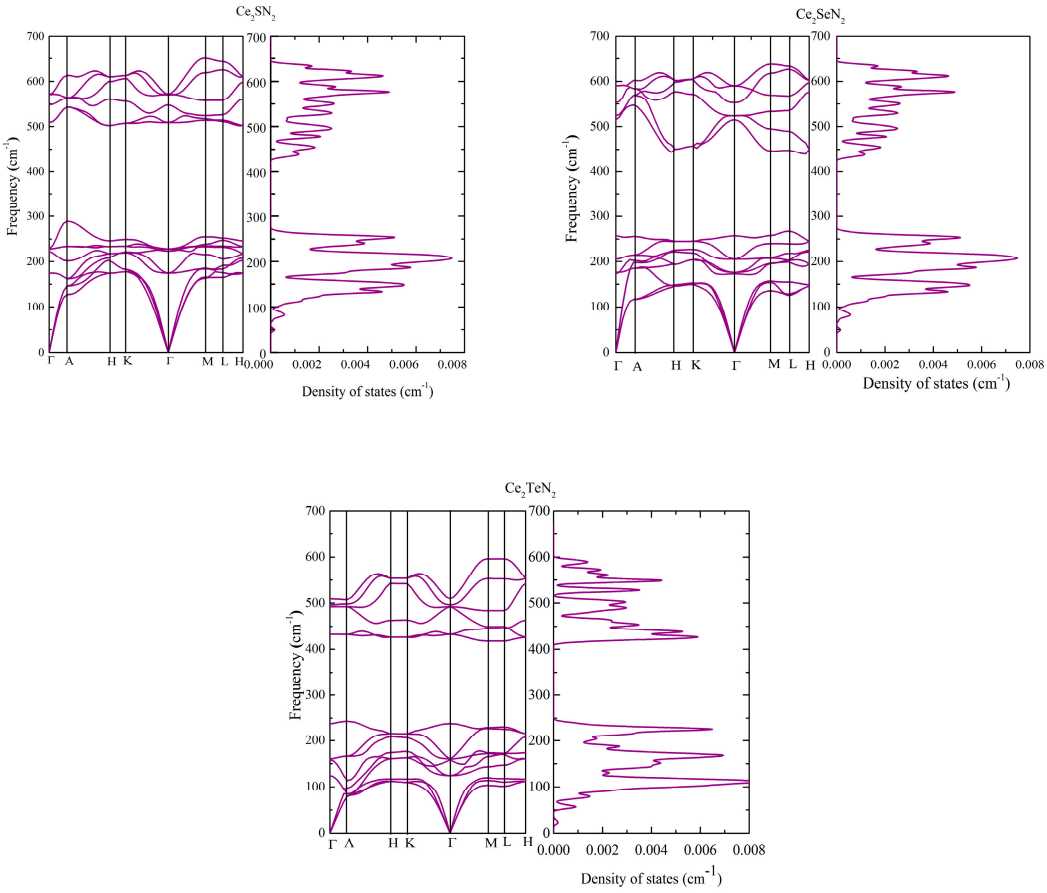

Figure 5. Calculated phonon dispersions along high-symmetry directions and Total phonon PDOS of Ce_2SN_2, Ce_2SeN_2, and Ce_2TeN_2.

4. Conclusions

In summary, we have studied the structural, electronic, and vibrational properties for new ternaries Ce_2SeN_2, Ce_2SN_2, and Ce_2TeN_2 using first-principles DFT+*U* calculation. It has been shown that the structural parameters determined after relaxation are in good agreement with the experimental data. Our predictions show that all ternaries are energetically and mechanically stable. Interestingly, we find from electronic structures DFT + *U* calculations that these chalcogenide nitrides are insulators. We also found that the binding in Ce_2XN_2 has a strong ionic character as well as a covalent nature due to the interaction between Ce f/*X* p and N p orbitals. We have also reported and discussed vibrational spectra. They show the dynamical stability of the considered nitrides.

Acknowledgments: Financial support for this study is acknowledged in the form of an internal grant IRG 16420 (M. B. Kanoun) and IRG 16417 (S. Goumri-Said) from office of research at Alfaisal University.

Author Contributions: Both authors have contributed in calculations and writing the manuscript.

Conflicts of Interest: The authors declare no conflict of interest.

References

1. DiSalvo, F.J.; Clarke, S.J. Ternary nitrides: A rapidly growing class of new materials. *Curr. Opin. Solid State Mater. Sci.* **1996**, *1*, 241–249.
2. Gregory, D.H. Nitride chemistry of the s-block elements. *Coord. Chem. Rev.* **2001**, *215*, 301–345.
3. Miura, A.; Wen, X.-D. ; Abe, H.; Yau, G.; DiSalvo, F.J. Non-stoichiometric Fe_xWN_2: Leaching of Fe from layer-structured $FeWN_2$. *J. Solid State Chem.* **2010**, *183*, 327–331.
4. Miura, A.; Tague, M.E.; Gregoire, J.M.; Wen, X.-D.; van Dover, R.B.; Abruna, H.D.; DiSalvo, F.J. Synthesis of Pt−Mo−N Thin Film and Catalytic Activity for Fuel Cells. *Chem. Mater.* **2010**, *22*, 3451–3456.
5. Foltin, M.L.; Schleid, T. The Short Series of Lanthanoid(III) Nitride Tellurides with the Composition Ln_3NTe_3 (*Ln* = Gd–Ho). *Z. Anorg. Allg. Chem.* **2015**, *641*, 292–297.
6. Schleid, T.; Lissner, F. $Cs_2Gd_6N_2Te_7$: The first quaternary nitride telluride of the lanthanides. *J. Alloys Compd* **2006**, *418*, 68–72.
7. Schleid, T.; Lissner, F. Lanthanido ammonium cations $[NM4]^{9+}$ as main structural features in lanthanide(III) nitride chalcogenides and their derivatives. *J. Alloys Compd* **2008**, *451*, 610–616.
8. Braunling, D.; Pecher, O.; Trots, D.M.; Senyshyn, A.; Zherebtsov, D.; Haarmann, F.; Niewa, R. Synthesis, Crystal Structure and Lithium Motion of Li_8SeN_2 and Li_8TeN_2. *Z. Anorg Allg. Chem.* **2010**, *636*, 936–946.
9. DiSalvo, F.J. Challenges and opportunities in solid-state chemistry. *Pure Appl. Chem.* **2000**, *72*, 1799–1807.
10. Miura, A.; Lowe, M.; Leonard, B.M.; Subban, C.V.; Masubuchi, Y.; Kikkawa, S.; Dronskowski, R.; Hennig, R.G.; Abrun, H.D.; DiSalvo, F.J. Silver delafossite nitride, $AgTaN_2$? *J. Solid State Chem.* **2011**, *184*, 7–11.
11. Dong, Y.; DiSalvo, F.J. Ce_2SeN_2: Ternary Selenide Nitride Containing Tetravalent Ce in the Ce_2SO_2 Structure Type. *Solid State Sci.* **2011**, *13*, 19–22.
12. Blochl, P.E. Projector augmented-wave method. *Phys. Rev. B* **1994**, *50*, 17953.
13. Kresse, G.; Furthmuller, J. Efficient iterative schemes for ab initio total-energy calculations using a plane-wave basis set. *Phys. Rev. B* **1996**, *54*, 11169.
14. Perdew, J.P.; Burke, K.; Ernzerhof, M. Generalized Gradient Approximation Made Simple. *Phys. Rev. Lett.* **1996**, *77*, 3865.
15. Liechtenstein, A.I.; Anisimov, V.I.; Zaanen, J. Density-functional theory and strong interactions: Orbital ordering in Mott-Hubbard insulators. *Phys. Rev. B* **1995**, *52*, R5467.
16. Kanoun, M.B.; Reshak, A.H.; Kanoun-Bouayed, N.; Goumri-Said, S. Evidence of Coulomb correction and spin-orbit coupling in rare-earth dioxides CeO_2, PrO_2 and TbO_2: An ab initio study. *J. Magn. Magn. Mater.* **2012**, *324*, 1397–1405.
17. Monkhorst, H.J.; Pack, J.D. Special points for Brillouin-zone integrations. *Phys. Rev. B* **1976**, *13*, 5188.
18. Bader, R.F. A quantum theory of molecular structure and its applications. *Chem. Rev.* **1991**, *91*, 893–928.
19. Holec, D.; Rachbauer, R.; Chen, L.; Wang, L.; Luef, D.; Mayrhofer, P.H. Phase stability and alloy-related trends in Ti–Al–N, Zr–Al–N and Hf–Al–N systems from first principles. *Surf. Coat. Technol.* **2011**, 206, 1698–1704.
20. Born, M.; Hang, K. *Dynamical Theory and Experiments I*; Springer Verlag Publishers: Berlin, Germany, 1982.
21. Hill, R. The Elastic Behaviour of a Crystalline Aggregate. *Proc. Phys. Soc.: Sect. A* **1952**, *65*, 349–354.
22. Holm, B.; Ahuja, R. Ab initio calculation of elastic constants of SiO_2 stishovite and α-quartz. *J. Chem. Phys.* **1999**, *111*, 2071–2074.
23. Goumri-Said, S.; Kanoun, M.B. DFT+*U* study of the oxide-ion conductor pentalanthanum hexamolybdenum henicosaoxide. *J. Solid State Chem.* **2013**, *197*, 304–311.
24. Azam, S.; Khan, S.A.; Goumri-Said, S. Exploring the electronic structure and optical properties of the quaternary selenide compound, $Ba_4Ga_4SnSe_{12}$: For photovoltaic applications. *J. Solid State Chem.* **2015**, *229*, 260–265.
25. Abadias, G.; Kanoun, M.B.; Goumri-Said, S.; Koutsokeras, L.; Dub, S.N.; Djemia, P. Electronic structure and mechanical properties of ternary ZrTaN alloys studied by ab initio calculations and thin-film growth experiments. *Phys. Rev. B* **2014**, *90*, 144107.
26. Clark, S.J.; Segall, M.D.; Pickard, C.J.; Hasnip, P.J.; Probert, M.J.; Refson, K.; Payne, M.C. First principles methods using CASTEP. *Zeitschrift für Kristallographie—Crystalline Materials* **2005**, *220*, 567–570.

27. Goumri-Said, S.; Kanoun-Bouayed, N.; Reshak, A.H.; Kanoun, M.B. On the electronic nature of silicon and germanium based oxynitrides and their related mechanical, optical and vibrational properties as obtained from DFT and DFPT. *Comput. Mater. Sci.* **2012**, *53*, 158–168.